applied optics

Single mode GaSb diode lasers for sensor applications in a long wavelength regime

Tobias Milde,[1,*] Christian Assmann,[1] Alvaro Jimenez,[1] Martin Honsberg,[2] James O'Gorman,[2,3] Wolfgang Schade,[4] and Joachim Sacher[1,2]

[1]Sacher Lasertechnik GmbH, Rudolf-Breitscheid-Str. 1-5, 35037 Marburg, Germany
[2]Sensor Photonics GmbH, Rudolf-Breitscheid-Str. 1-5, 35037 Marburg, Germany
[3]Xylophone Optics Ltd., Vanomer House, 191-195 Lower Kimmage Rd., Dublin 6W, Ireland
[4]Technische Universität Clausthal, Am Stollen 19a, 38640 Goslar, Germany
*Corresponding author: tobias.milde@sacher-laser.com

Received 31 May 2017; revised 15 August 2017; accepted 18 August 2017; posted 18 August 2017 (Doc. ID 297147); published 8 September 2017

The wavelength, λ, range of 1.8 μm $\leq \lambda \leq$ 3.5 μm contains strong spectral absorption lines of many gases used in health, industry, safety, and medicine and whose sensitive and quantitative detection is desirable. However, the performance of InP diode lasers markedly deteriorates beyond $\lambda\sim$2 μm. In this paper we present new results on developing tunable high power single mode laser diodes based on the GaSb material system with emission in the wavelength range of 1.8 μm $\leq \lambda \leq$ 2.2 μm.

OCIS codes: (140.2020) Diode lasers; (140.3070) Infrared and far-infrared lasers; (140.3380) Laser materials; (140.3490) Lasers, distributed-feedback; (140.3570) Lasers, single-mode; (140.3600) Lasers, tunable.

https://doi.org/10.1364/AO.56.000H45

1. INTRODUCTION

Tunable diode laser absorption spectroscopy (TDLAS) is a versatile and robust method for gas sensing with applications ranging in industry, health and safety (e.g., toxic gas, alcohol, and explosives), and medicine [1–3]. Gallium antimonide (GaSb) is an important material system for single mode diode lasers for the near and mid-infrared spectral region. While it is well known that beyond $\lambda \sim$ 1.8 μm, GaSb shows higher gain and offers higher power than lasers grown on an indium phosphide (InP) material system [4], only a few reports have described the fabrication of single mode laser diodes targeting the spectral range of 1.8 μm $\leq \lambda \leq$ 2.2 μm with GaSb materials. Here we present the advantages of GaSb based lasers in the 2 μm regime where we do not know existing publications, and we report on the design and growth of epitaxial structures as well as on their performance when fabricated into GaSb laser diodes [5] in this regime. All common publications of our knowledge have concentrated on the spectral range of 2.3 μm $\leq \lambda \leq$ 3 μm with the GaSb material system [6–8] and below 2.3 μm with the InP material system [9]. In addition, a summary of 35 potential biomarkers and their physiological symptoms is presented as an application example in [1]. Here we present, to the best of our knowledge, the first application data of fabricated single mode GaSb laser devices on N_2O (nitrous oxide or laughing gas), CO_2 (carbon dioxide), and H_2O (water vapor) in the 1.9 μm $\leq \lambda \leq$ 2.1 μm spectral regions.

2. EPITAXIAL STRUCTURE OF GASB BASED SINGLE MODE LASER DIODES

The goal of our research reported here is to develop new cost-effective laser diode sources with higher power than currently provided by InP based laser diodes emitting in the 1.8 μm $\leq \lambda \leq$ 3.5 μm wavelength range, enabling higher detection sensitivities of industrially interesting gases. Overcoming the shortcomings of existing wavelength tunable laser diodes and negating their underlying deficiencies has driven our design and development of low-cost single mode laser diodes with emission in the wavelength range of 1.8 μm $\leq \lambda \leq$ 3.5 μm. The cost and detection sensitivity issues have been simultaneously addressed by exploiting new lower-cost and more easily manufactured laser diode devices, digital distributed feedback (DFB) laser diodes, where single mode emission is obtained by etching a digital grating in the upper surface of a conventional ridge waveguide (RWG) Fabry–Perot (FP) laser to provide single mode lasers at these longer wavelengths with high emission power and narrow emission lines with high side mode suppression ratios (SMSRs). Digital DFB laser diodes (D-DFBs) use digital gratings that are photo-lithographically patterned directly along the upper surface of an otherwise conventional RWG FP laser. This approach requires only a single material growth stage and uses optical lithography and simple etching to realize both the ridge and digital grating [10]. Our long wavelength GaSb laser diodes are fabricated using compressively strained GaSb wafers as shown in the structure in Table 1.

Table 1. Typical Layer Structure of the Grown GaSb Single Mode Diode Lasers

Material	*x*	*y*	Thickness (µm)
GaSb			0.3
AlxGa1-xAsySb1-y	0.6	0.052	1.5
AlxGa1-xAsySb1-y	0.24	0.02	0.3
Ga1-xInxSb	0.2		0.008
AlxGa1-xAsySb1-y	0.24	0.02	0.015
Ga1-xInxSb	0.2		0.008
AlxGa1-xAsySb1-y	0.24	0.02	0.015
Ga1-xInxSb	0.2		0.008
AlxGa1-xAsySb1-y	0.24	0.02	0.3
AlxGa1-xAsySb1-y	0.6	0.052	1.5

Figure 1 shows the room temperature photoluminescence (PL) spectra of the grown GaSb wafers whose typical layer structure is displayed in Table 1. The wafers are designed for optimized peak PL emission at $\lambda = 1.9$ nm and $\lambda = 2.02$ µm. Excellent agreement is seen between the designed and realized PL peak emission. The features on the short wavelength shoulder of the spectrum labeled $\lambda = 1.896$ nm are due to absorption by water vapor in the PL measurement apparatus. The PL spectra are otherwise characterized by excellent intensity and a smooth distribution of power across the wavelength spectrum.

To process the wafer further for chip manufacturing, RWG and grating structures are etched into the wafer material. Simulations were carried out to refine the etch depth and waveguiding properties of RWG structures to be implemented in the layer structure. This is illustrated in Fig. 2, while Fig. 3 shows the calculated far-field patterns of the mode that is guided under the waveguide. The material loss is deduced from the overlap of the mode with the individual layers and mainly affected by the p-doping profile [11].

Using this data, simulations were carried out on the lasing characteristics of different devices of varying length and facet reflectivities, as shown in Fig. 4. The different chip lengths used are $L_{cav} = 400$, 600, and 900 µm. For the diode laser facets, one side was kept constant at a high reflectivity value of 90%

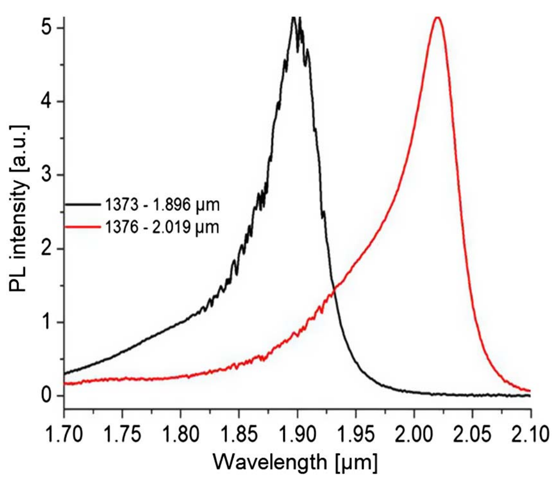

Fig. 1. Measured photoluminescence spectrum of GaSb layer structure of Table 1.

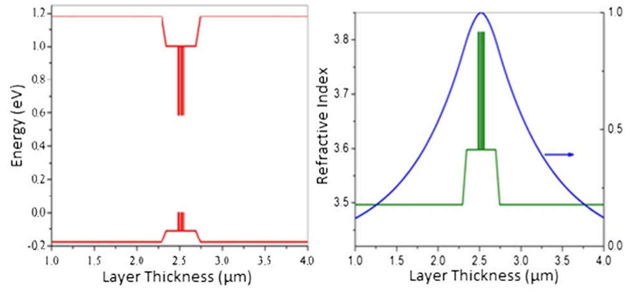

Fig. 2. Simulated layer thickness and its effect on the guided mode.

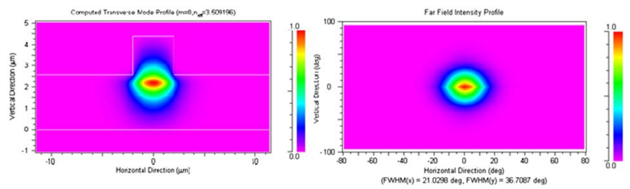

Fig. 3. Calculated far-field patterns of the mode guided under the waveguide.

while the other one was varied between 1% and 20% [12,13]. Figure 5 shows the measured light-intensity (L) versus bias current (I), L versus I, curves for a range of L_{cav} as delineated in the figure and for facet reflectivities of 90% and 10%. These simulations are encouraging, as they project that a reasonable emission power can be obtained even with short devices.

Simulations follow the same trend as before, also taking into account that the internal losses due to the wavelength selection elements will be considerably higher. The results are presented in the same way as the previous L versus I curves, accounting for different chip lengths and a constant reflectivity [14] for the diode's facet, as can be seen in Fig. 6. The measured LI curve for the single tunable mode is displayed in Fig. 7.

3. RESULTS AND APPLICATION DATA

The National Meteorological Service of Germany, the Deutscher Wetterdienst (DWD), defines H_2O, CO_2, CH_4,

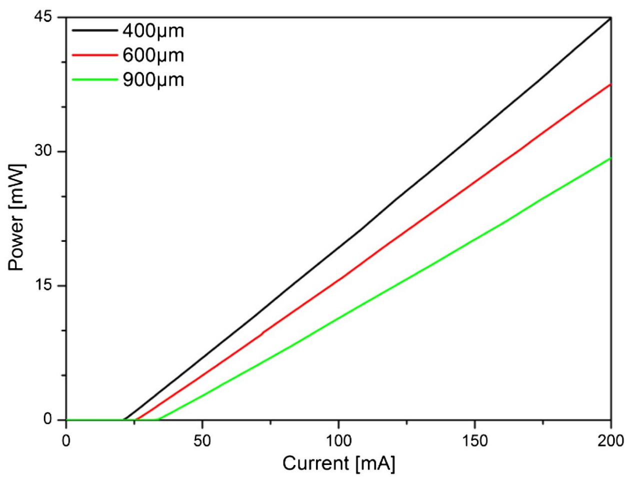

Fig. 4. Calculated L versus I curves for different FP chip lengths.

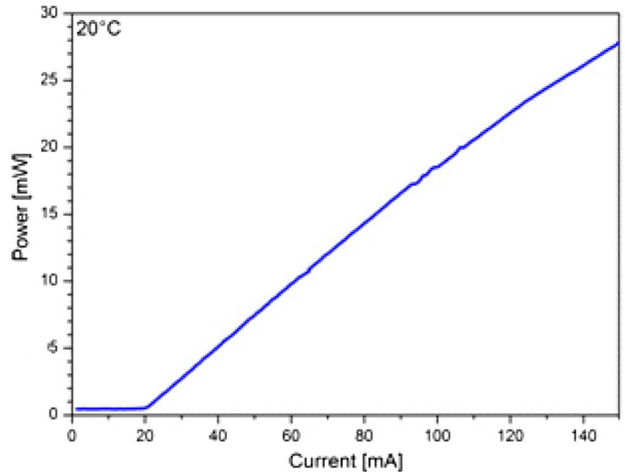

Fig. 5. Measured L versus I curve for an FP chip of length $L_{cav} = 400$ µm.

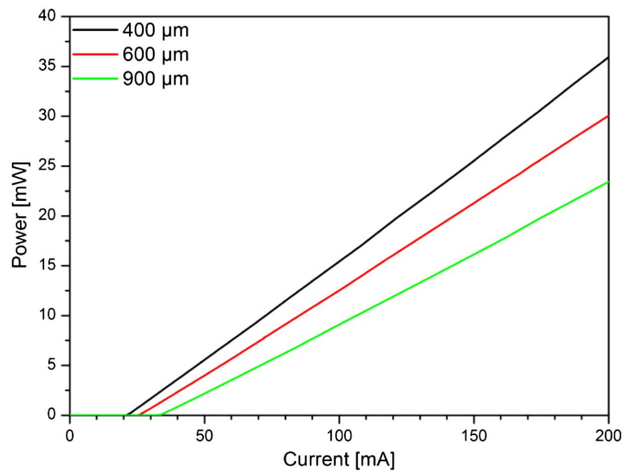

Fig. 6. Calculated L versus I curves for different chip lengths in a single mode tunable mode configuration.

and N_2O as the most concerning greenhouse gases. As water vapor is the most problematic one, because of its quantity in the atmosphere, due to the fact that it has its own natural sources, the other three are already much more effective in lower doses [15].

In this paper we concentrate on the detection of H_2O, N_2O, and CO_2 as applications for the new long wavelength excitation sources. The used wavelength range was 1.88 µm $\leq \lambda \leq$ 2.13 µm. Furthermore, N_2O and CO_2 are two very important gases in the area of biomedical patient monitoring and treatment. CO_2 is a monitoring gas especially for breath analysis, and N_2O is a gas used in anesthesia.

For the experimental setup, different excitation sources were selected for all the gases of interest. All laser diodes are specified in the following subsections with their sensor applications. The laser diodes are temperature stabilized, and for these measurements the submount temperatures, T_{LD}, were controlled with a precision of $T_{LD} = 20°C \pm 0.01°C$. For sensor applications,

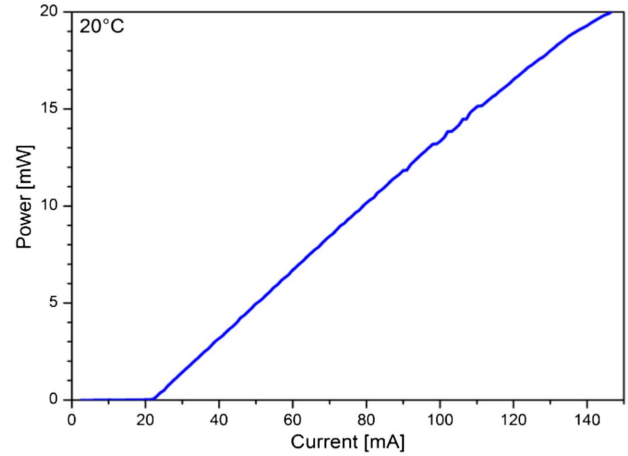

Fig. 7. Measured L versus I curve for a 400 µm chip length in single tunable mode configuration.

the measurements were done by projecting the laser light through a 1-m-long gas tube where several gas values can be controlled. In these experiments the tube was not heated or cooled so that the gas was held at room temperature. After the gas tube the optical signal was measured using an extended response InGaAs detector specified for these wavelengths.

A. GaSb DFB Diode Laser with Emission Around λ~2 µm for Use in a CO_2 Sensor Application

While CO_2 is a greenhouse gas, it is also interesting in the medical area for applications such as breath monitoring. CO_2 has multiple absorption lines around $\lambda \sim 2$ µm. We packaged a digital DFB diode with emission centered at λ~2 µm to measure the detectivity of CO_2 using these devices at λ~2 µm. The characteristics of this diode are shown in Fig. 8.

As can be seen in Fig. 8, the laser threshold is around 20 mA and the laser emission power increases with bias current to

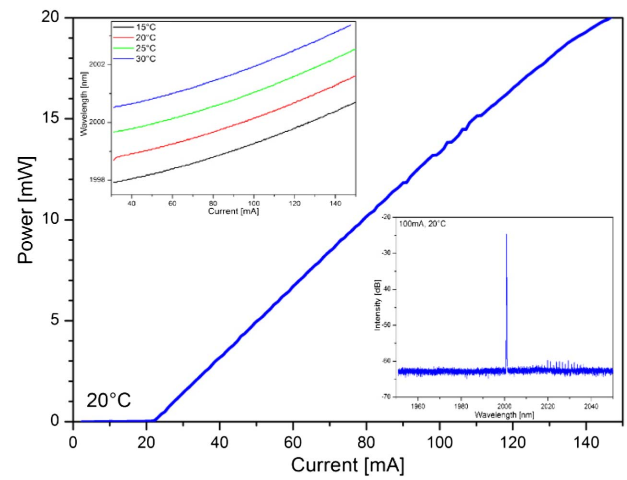

Fig. 8. L versus I versus I curve for the λ~2 µm GaSb digital DFB laser diode. The wavelength tuning behavior with bias current can be seen in the upper inset for different temperatures. In the lower inset the measured optical spectrum is shown, with an SMSR value of 35.59 dB.

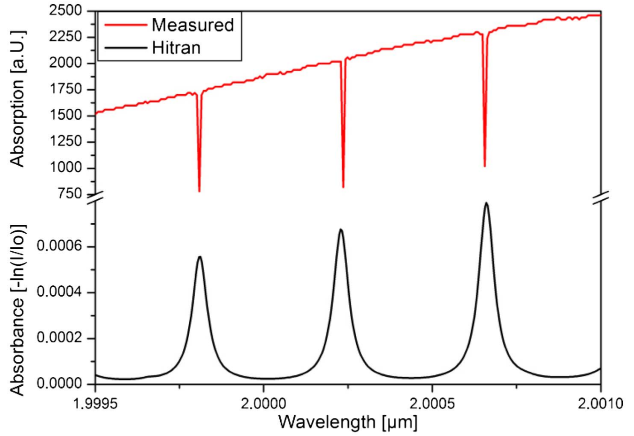

Fig. 9. Measured ro-vibrational R15 to R17 states of CO_2 in the range of 1999.5 to 2001 nm at 4.5 mbar (red curve); calculated HITRAN spectrum by spectraplot.com [16] (black curve) under the same conditions.

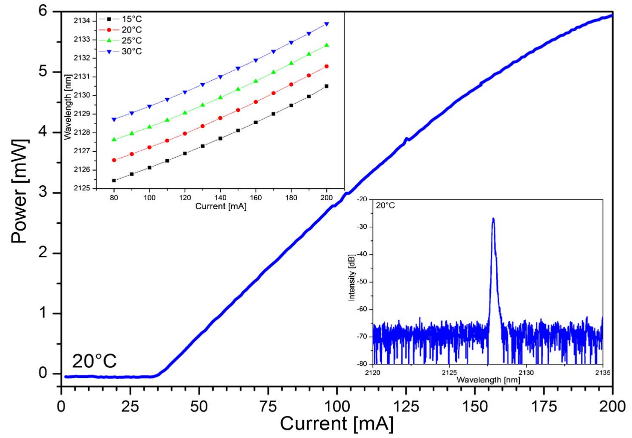

Fig. 10. L versus I versus I curve of the λ~2.114 μm digital DFB laser diode at $T_{LD} = 20°C$. The behavior with bias current can be clearly seen in the upper inset for different temperatures. In the lower inset the emission spectrum is plotted and the optical spectrum. An SMSR of 36.7 dB is measured, limited by the sensitivity of the optical spectrum analyzer.

almost 20 mW at $I = 140$ mA. In the lower inset the optical spectrum is shown. The measured (instrument limited) SMSR is 35.59 dB at $I_{\text{bias}} = 100$ mA (corresponding to an emitted power of P_{out}~10 mW). In the upper inset the tuning behavior of the wavelength over the current is displayed for four different temperatures in steps of 5 deg. The current tuning range is around $\Delta\lambda = 2$ nm for ΔI_{bias}~100 mA. The temperature tuning range is about $\Delta\lambda = 2.5$ nm for $\Delta T_{LD} = 15$ deg. By varying the laser bias current around 110 mA with a 75 mA peak to peak sinusoidal modulation current, the gas absorption was scanned over a wavelength range of 1.5 nm. The measured CO_2 spectrum is displayed in Fig. 9 (red curve), where the ro-vibrational states of CO_2 can be seen. Here the R15 to R17 states are measured with the λ~2 μm digital DFB laser emission. For comparison in Fig. 9 the simulated HITRAN spectrum [16] is displayed (black curve). As is clear, the measured and the simulated spectra match quite well. In the experiment as well as in the simulation the pressure of the gas tube was set to 4.5 mbar (3.3 Torr; 450 Pa).

B. 2128 nm DFB Diode Laser as Sensor Application for N_2O

The detection of N_2O (laughing gas) can also be interesting in the concern of greenhouse gases as well as for medical monitoring of laughing gas as a narcotic gas for surgeries. N_2O has a broad ro-vibrational absorption comb around λ~2.114 μm that ranges over 25 nm to both sides [16]. For measuring this gas we packaged a GaSb diode with a central wavelength of λ~2.128 μm from a comparable wafer as done previously. This shows the flexibility of the technology since many different laser diodes with different emission wavelengths can be implemented using a single mask set. The characteristics of this λ~2.128 μm digital DFB laser diode are shown in Fig. 10.

In Fig. 10 the light-intensity behavior is displayed. There it is shown that the laser threshold is around 35 mA and that the laser power can be increased by increasing the laser bias current to a maximum of $P_{\text{out}} = 6$ mW at $I_{\text{bias}} = 200$ mA. In the upper inset the wavelength tuning behavior over the current is displayed for different temperatures. The current tuning range is nearly $\Delta\lambda = 5$ nm for $\Delta I_{\text{bias}} = 120$ mA. The temperature tuning range is over 3 nm for $T_{LD} = 15°C$. In the lower inset the optical spectrum is shown. An instrument limited SMSR of 36.7 dB is measured for $I_{\text{bias}} = 110$ mA. The lower output power and the higher threshold compared with the 2 μm DFB laser are caused by an earlier development stage where the RWG topology and surface roughness were not as ideal as in the 2 μm wafer. Also the reflectivity of the front facet coating is 30% instead of 10% for the 2 μm DFB laser [17].

The gas absorption was measured over a wavelength range of 2 nm by tuning the laser around 150 mA with a peak to peak sinusoidal modulation current of 48 mA at normal conditions. The measured N_2O spectrum is displayed in Fig. 11 (red curve), where the ro-vibrational states of N_2O can be clearly observed. Here the P33 to P35 states are measured with the

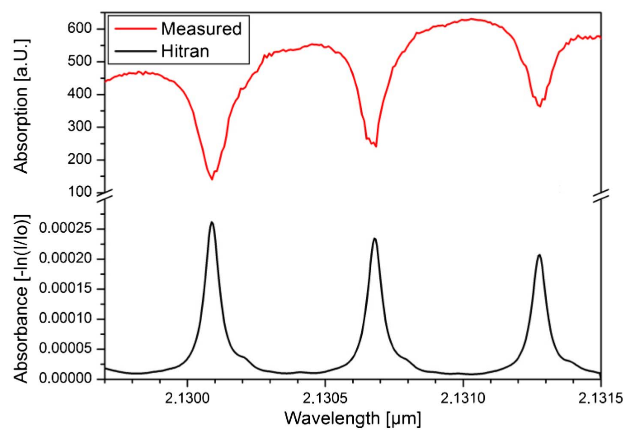

Fig. 11. Measured ro-vibrational P33 to P35 states of N_2O in the wavelength range of 2129.7 nm $\le \lambda \le$ 2131.5 nm (red curve); calculated HITRAN spectrum by spectraplot.com [16] (black curve) under the same conditions.

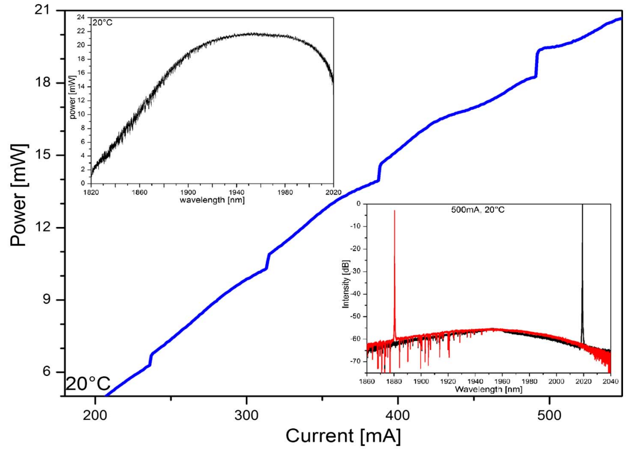

Fig. 12. PI curve of the 1.95 μm ECDL at the central wavelength. The motor tuning behavior and with it the power to wavelength correlation is shown in the upper inset. In the lower inset the optical spectrum is displayed for both extremes of the tuning behavior with an SMSR value of 52.4 dB at 1.88 μm and 55 dB at 2.02 μm.

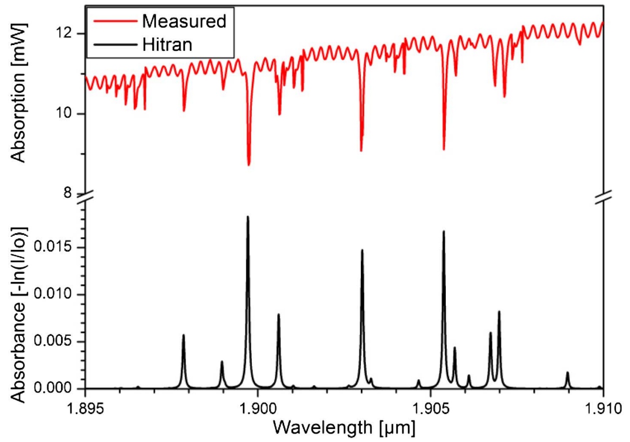

Fig. 13. Measured absorption states of water vapor in the wavelength range of 1.895 μm $\leq \lambda \leq$ 1.91 μm nm (red curve); calculated HITRAN spectrum by spectraplot.com [16] (black curve) under the same conditions.

$\lambda = 2.128$ μm digital DFB laser. Again for comparison in Fig. 11 (black curve), the simulated HITRAN spectrum [16] is displayed. As can be seen, the measured and the calculated spectra show good accordance.

C. $\lambda = 1950$ nm External Cavity Diode Laser as Water Vapor Sensor Application

Water vapor is the most important greenhouse gas because of its quantity in the atmosphere. Water vapor also has huge natural sources, as sunlight has only to shine on the oceans to increase the water vapor concentration. Strong water vapor absorption lines are distributed over the whole IR spectral region, thereby making the measurement quite straightforward. Indeed the absorption lines were so strong that a gas tube was not required and just beaming the laser a few centimeters through the laboratory air at normal conditions sufficed to measure strong absorption. This measurement was also done with another type of laser source than the devices used before. Here we utilized an external cavity diode laser (ECDL) arrangement that was emitted in a narrow spectrum when operated in the Littman configuration [18,19]. In a Littman configuration the wavelength can be tuned by adjusting the mirror position relative to the grating by a motor. For measuring water vapor we used a GaSb diode based ECDL where the GaSb FP gain block operated at a center wavelength of $\lambda \sim 1.95$ μm. The emission characteristics of this ECDL are shown in Fig. 12.

The laser threshold is $I_{\text{bias}} = 112$ mA, and the laser power can be increased with bias current to a maximum of nearly 21 mW, both at the central wavelength of 1.95 μm. The kinks in the PI curve are mode hops, which result from chip length changes with increasing laser current [17,20]. In the lower inset the optical spectrum is shown. A stable SMSR value exceeding 50 dB is seen at $I_{\text{bias}} = 500$ mA for the entire tuning range. The tuning behavior of the wavelength by the external cavity can also be seen in both insets of Fig. 12. In the upper inset the power output over the motor tuning behavior is displayed. By adjusting the mirror in this Littman configuration, the motor can tune the wavelength from 1.82 to 2.02 μm.

By tuning the wavelength of the ECDL with the motor the gas was scanned over a wavelength range of 15 nm. The measured H_2O spectrum is displayed in Fig. 13 (red curve).

Here the used detector was a power meter, which also displays the power behavior of the ECDL when wavelength tuned. A trend of increasing power can be noticed due to this effect. For comparison, in Fig. 13 the simulated HITRAN spectrum [16] (black curve) is displayed. As can be seen, the measured and the simulated spectra again match quite well.

4. CONCLUSIONS

The successfully fabricated GaSb based D-DFB and ECDL systems are a milestone for the sensing of markers for medical diagnosis and greenhouse monitoring. Future work will expand the wavelength coverage into the wavelength range of 1.8 μm $\leq \lambda \leq$ 3.4 μm. Many molecular gases, which are relevant for gas sensing with applications ranging in health and safety (e.g., toxic gas, alcohol, and explosives), industry, and medicine, show significant absorption within this spectral region [16]. Here we provided examples demonstrating the excellent performance of GaSb grown diode laser systems with high power performance and excellent single mode behavior, proving their high capability for future application. This excellent performance was verified via spectroscopy of relevant greenhouse gases and gases of medical interest.

Funding. Bundesministerium für Bildung und Forschung (BMBF) (13N13822, 13N13823).

REFERENCES

1. C. Wang and P. Sahay, “Breath analysis using laser spectroscopic techniques: breath biomarkers, spectral fingerprints, and detection limits,” Sensors **9**, 8230–8262 (2009).
2. R. Liang, J. Chen, G. Kipshidze, D. L. Shterengas, and G. Belenky, “High-power 2.2 μm diode lasers with heavily strained active region,” IEEE Photon. Technol. Lett. **23**, 603–605 (2011).

3. Y.-Z. Song, Y. Zhang, J.-K. Song, K.-W. Li, Z.-Y. Zhang, Y. Xu, G.-F. Song, and L.-H. Chen, “Single mode 2 μm GaSb based laterally coupled distributed feedback quantum-well laser diodes with metal grating,” Chin. Phys. Lett. **32**, 074206 (2015).
4. “Semiconductor database of Ioffe Inst. St. Petersburg,” http://www.ioffe.ru/SVA/NSM/Semicond/
5. T. Milde, A. Jimenez, J. R. Sacher, and J. O’Gorman, “Long wavelength single mode GaSb diode lasers for sensor applications,” in *Conference on Lasers and Electro-Optics*, OSA Technical Digest (Optical Society of America, 2017), paper JTu5A.111.
6. D. Sanchez, L. Cerutti, and E. Tournié, “Single-mode monolithic GaSb vertical-cavity surface-emitting laser,” Opt. Express **20**, 15540–15546 (2012).
7. J. A. Gupta, P. J. Barrios, J. Lapointe, G. C. Aers, and C. Storey, “Single-mode 2.4 μm InGaAsSb/AlGaAsSb distributed feedback lasers for gas sensing,” Appl. Phys. Lett. **95**, 041104 (2009).
8. Q. Gaimard, M. Triki, T. Nguyen-Ba, L. Cerutti, G. Boissier, R. Teissier, A. Baranov, Y. Rouillard, and A. Vicet, “Distributed feedback GaSb based laser diodes with buried grating: a new field of single frequency sources from 2 to 3 μm for gas sensing applications,” Opt. Express **23**, 19118–19128 (2015).
9. J. A. Nwaboh, O. Werhahn, P. Ortwein, D. Schiel, and V. Ebert, “Laser-spectrometric gas analysis: CO_2–TDLAS at 2 μm,” Meas. Sci. Technol. **24**, 015202 (2013).
10. A. Jimenez, T. Milde, N. Staacke, C. Assmann, J. O’Gorman, and J. Sacher, “Narrow-line diode laser packaging and integration in the NIR and MIR spectral range,” Proc. SPIE **10085**, 1008505 (2017).
11. M. Rattunde, J. Schmitz, R. Kiefer, and J. Wagner, “Comprehensive analysis of the internal losses in 2.0 mm (AlGaIn)(AsSb) quantum-well diode lasers,” Appl. Phys. Lett. **84**, 4750–4752 (2004).
12. J. Sacher, W. Elsässer, and E. O. Göbel, “Nonlinear dynamics of semiconductor laser emission under variable feedback conditions,” IEEE J. Quantum Electron. **27**, 373–379 (1991).
13. M. V. Bogdanovich, V. V. Kabanov, Y. V. Lebiadok, A. G. Ryabtsev, G. I. Ryabtsev, M. A. Shchemelev, S. S. Kurlenkov, S. M. Sapozhnikov, and S. K. Mehta, “Optimal output mirror reflection coefficient for powerful InGaAs/AlGaAs laser diode arrays,” Opt. Laser Technol. **45**, 177–180 (2013).
14. J. Sacher, D. Baums, P. Panknin, W. Elsässer, and E. O. Göbel, “Intensity instabilities of semiconductor lasers under current modulation, external light injection, and delayed feedback,” Phys. Rev. A **45**, 1893–1905 (1992).
15. “DWD website to climate gases,” http://www.dwd.de/EN/research/observing_atmosphere/composition_atmosphere/trace_gases/cont_nav/climate_gases.html.
16. “HITRAN spectra simulation website,” http://spectraplot.com.
17. A. Jiménez, T. Milde, N. Staacke, C. Assmann, G. Carpintero, and J. Sacher, “Narrow-line external cavity diode laser micro-packaging in the NIR and MIR spectral range,” Appl. Phys. B **123**, 207 (2017).
18. S. Stry, S. Thelen, J. Sacher, D. Halmer, P. Hering, and M. Mürtz, “Widely tunable diffraction limited 1000 mW external cavity diode laser in Littman/Metcalf configuration for cavity ring-down spectroscopy,” Appl. Phys. B **85**, 365–374 (2006).
19. L. Hildebrandt, R. Knispel, S. Stry, J. Sacher, and F. Schael, “Antireflection-coated blue GaN laser diodes in an external cavity and Doppler-free indium absorption spectroscopy,” Appl. Opt. **42**, 2110–2118 (2003).
20. S. Rauch and J. Sacher, “Compact Bragg grating stabilized Ridge waveguide laser module with a power of 380 mW at 780 nm,” IEEE Photon. Technol. Lett. **27**, 1737–1740 (2015).